Journal of Southeast University (English Edition) Vol. 30, No. 3, pp. 330 - 335 Sept. 2014 ISSN 1003—7985

Experimental and numerical study on flexural behaviors of steel reinforced engineered cementitious composite beams

Cai Jingming Pan Jinlong Yuan Fang

(Key Laboratory of Concrete and Prestressed Concrete Structures of Ministry of Education, Southeast University, Nanjing 210096, China)

Abstract: To investigate the flexural behaviors of steel reinforced engineered cementitious composite (ECC) beams, the behaviors of the steel reinforced ECC beam and the conventional steel reinforced concrete beam subjected to flexural load are experimentally compared. The experimental results show that the flexural strength and ductility of the steel reinforced ECC beam are 24.8% and 187.67% times larger than those of the steel reinforced concrete beam, and the substitution of concrete with ECC can significantly delay the propagation of cracks. Additionally, a simplified constitutive model of the ECC material is used to simulate the flexural behaviors of beams by the finite element analysis (FEA). The results show a good agreement between the simulation and test results. The crack width of the steel reinforced ECC beam can be limited to 0.4 mm under the service load conditions. The application of ductile ECC can significantly increase the flexural performance in terms of flexural strength, deformation capacity and ductility of the beams.

Key words: engineered cementitious composites (ECC); ductility; flexural behavior; finite element

doi: 10.3969/j.issn.1003-7985.2014.03.014

Concrete is a type of composite material with a high compressive strength and good bond strength with steel reinforcement, which makes it one of the most widely used materials in construction engineering[1]. However, concrete has low tensile strength and can become brittle, which results in low ductility and poor durability[2]. In recent years, a class of high performance fiber reinforced cementitious composites (called engineered cementitious composites, ECC) with ultra-ductility has been developed for applications in the construction industry[3-4]. ECC and concrete have similar ranges of tensile strength (4 to 6 MPa) and compressive strength (30 to 80 MPa)[5], but they behave differently in tension. For conventional concrete, it becomes brittle once the first localized crack is formed. However, for an ECC member under uniaxial tension, after the first cracking, the tensile load capacity continues to increase. The strain hardening behavior is accompanied by the formation of multiple cracks and the crack width of the ECC member can be limited to a considerable low value.

Up to now, many experimental studies have been conducted on the mechanical performance of steel reinforced ECC members, including coupling beams[6], columns[7], column-beam connections[8], infill panels[9], frames[10], precast bridge column[11], etc. However, limited effective numerical simulations have been conducted to study the structural behaviors of steel reinforced ECC members.

In this paper, a pair of steel reinforced beams are tested to verify the contribution of the ECC material to the flexural properties of the beams. The influence of matrix types on the ultimate strength, deformation capacity and ductility are evaluated. The flexural behaviors of the beams are numerically modeled with the finite element software ATENA. The comparisons of strain distribution, crack patterns, and crack width development between reinforced concrete (RC) beams and reinforced ECC (R/ECC) beams are also studied.

1 Experimental Program

1.1 Material properties

In order to enhance the environmental sustainability of the ECC, a high volume fraction (80%) of fly ash was employed in the cementitious binder in this study. Tab.1 shows the mixture proportions of the ECC material and concrete. According to the uniaxial tension tests, the tensile strength of the ECC materials exceeds 5 MPa and the ultimate tensile strain approaches 4%. A number of cylinder specimens, 100 mm in diameter and 200 mm in height, were also prepared with concrete and the ECC, and tested in compression. The compressive strength of the ECC and concrete were 38.3 and 47.2 MPa, respectively; while the elastic modulus of the ECC and concrete were 15.50 and 34.49 GPa, respectively. For each beam specimen, the steel bar with the diameter of 20 mm was used as the tensile reinforcement. The steel reinforcement with the diameter of 8 mm was employed as the compression reinforcement and supports for the hanging of the

Received 2014-02-26.

Biographies: Cai Jingming (1989—), male, graduate; Pan Jinlong (corresponding author), male, doctor, professor, jinlongp@gmail.com.

Foundation items: The National Natural Science Foundation of China (No. 51278118), the National Basic Research Program of China (973 Program) (No. 2009CB623200), the Natural Science Foundation of Jiangsu Province (No. BK2012756).

Citation: Cai Jingming, Pan Jinlong, Yuan Fang. Experimental and numerical study on flexural behaviors of steel reinforced engineered cementitious composite beams[J]. Journal of Southeast University (English Edition), 2014, 30(3): 330 - 335. [doi: 10.3969/j.issn.1003-7985.2014.03.014]

stirrups along the beam. Tab. 2 shows the mechanical properties of steel bars.

Tab. 1 Mixture proportions of cementing material %

Matrix	φ (sand)	φ (PVA fiber)	φ (water)	φ (water reducer)	φ (coarse aggregate)
ECC	20	2	22	80	
Concrete	15		35	30	25

Tab. 2 Material properties of steel reinforcement

Diameter/mm	Yield strength f_y/MPa	Ultimate strength f_u/MPa	Ultimate stain ε_{su}	Modulus of elasticity E_s/GPa
8	460	600	0.08	200
20	470	615	0.08	204

1.2 Specimen details and loading configuration

Two beam specimens with the dimension of 200 mm (width) × 300 mm (height) × 2 350 mm (length) are tested to investigate the flexural behaviors. One is steel reinforced ECC (R/ECC) beam, and the other is steel reinforced concrete (RC) beam for comparison. Dense stirrups with the diameter of 8 mm and the spacing of 100 mm are arranged in a shear span to avoid brittle shear failure of beams. Each beam is loaded under four-point bending with a span of 2 050 mm between supports, and loading is applied symmetrically at 850 mm from the supports. The loading configuration is shown in Fig. 1.

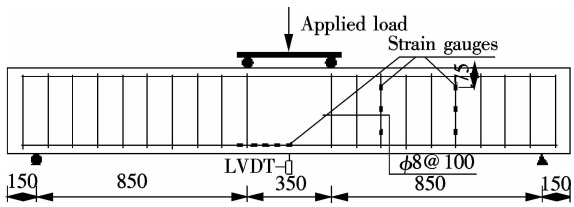

Fig. 1 Schematic illustration of test setup and specimen details (unit: mm)

A linear variable differential transformer (LVDT) was employed to monitor the mid-span deflection of the beam. To measure the strain variations of the steel reinforcement, a number of strain gauges were attached to the longitudinal tensile bars at a spacing of 50 mm and on two stirrups at a spacing of 75 mm. For the two stirrups, one is 375 mm from the middle span, and the other is 675 mm from the middle span. The distribution of strain gauges is shown in Fig. 1. The beams are loaded up to failure (corresponding to 80% of its peak load), followed by an unloading process to obtain the elastic energy. The data from strain gauges, LVDTs and load cell are automatically collected by a data logger.

2 Experimental Results and Discussion

2.1 Load-deflection responses and failure modes

According to the test results, the ultimate load capacity of the RC beam is 168.5 kN with a mid-span deflection of 19.2 mm. After that, the loading keeps constant with further increasing deflections at the two loading points. Finally, the RC beam is failed by the crushing of concrete in compression zone. For the R/ECC beam, the flexural load capacity reaches an applied load of 210.4 kN, which is 24.8% larger than that of the RC beam (see Fig. 2). In the ultimate stage, hundreds of tiny cracks are observed with a crack spacing of about 6 to 8 mm for the R/ECC beam, while only about 8 evident flexural or shear cracks are observed along the beam span for the RC beam. The final crack pattern is shown in Fig. 3(a). The results indicate that the substitution of concrete with the ECC for the steel reinforced beam can significantly decrease crack width and improve the flexural stiffness of the beam, resulting in high post-peak strength and energy absorption of the beam. The final crack pattern of the R/ECC beam is shown in Fig. 3(b). Compared with the RC beam, it has the superior compressive deformation capacity of the ECC that avoids premature failure of the R/ECC beam and improves ductility consequently.

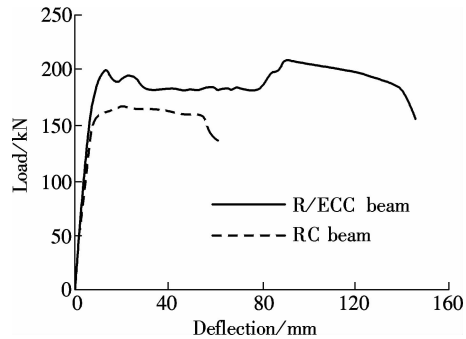

Fig. 2 Load-deflection curves of beam specimens

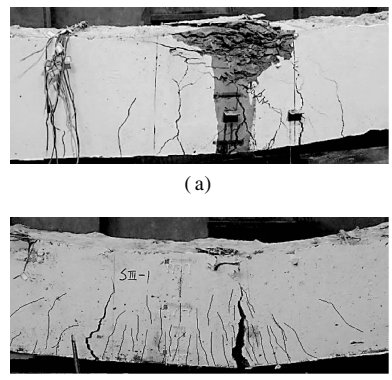

(a)

(b)

Fig. 3 Failure modes and crack patterns. (a) RC beam; (b) R/ECC beam

2.2 Strain analysis

Fig. 4 shows the strain distributions along the longitudinal reinforcement of specimens at different load levels. For the RC beam, the premature flexural cracks occurred along the RC beam, leading to strain fluctuations along the longitudinal reinforcement. In contrast, for the R/ECC beam, the strains distribute uniformly along the lon-

gitudinal reinforcement due to the formation of multiple fine cracks along the beam. For each load value, the strains along the longitudinal reinforcement in the RC beams are much larger than those in R/ECC beams. This is due to the superior tensile ductility of ECC and the good deformation compatibility between steel reinforcement and ECC when inelastic deformation occurs. Fig. 5 shows the comparison of average stirrup strains at two different locations for specimens. Since both beams fail in the flexural mode, the strain values for all stirrups do not exceed the steel yield strain. However, the strain development is distinctly different for the two beams. It can be observed from Fig. 5 that the strain values of the RC beam fluctuates around zero before the applied load reaches around 70 kN (when the first crack occurs in this section). For the ECC beam, the strain values fluctuates around zero before the applied load reaches about 110 kN, indicating that the substitution of concrete with the ECC can significantly delay the propagation and opening of cracks in the beam. With further loading, the strain values along the stirrups increase quickly but the strain values for the ECC beam are much lower than those of the concrete beam under the same load. Once cracks are formed in the concrete beam, the shear resistance is significantly reduced. However, for the ECC beam, the formation of multiple fine cracks (rather than discrete cracks with large opening) enables the shear resistance to be maintained under further loading. As a result, the substitution of concrete with ECC in a flexural member can significantly improve its load and deformation capacity under shear.

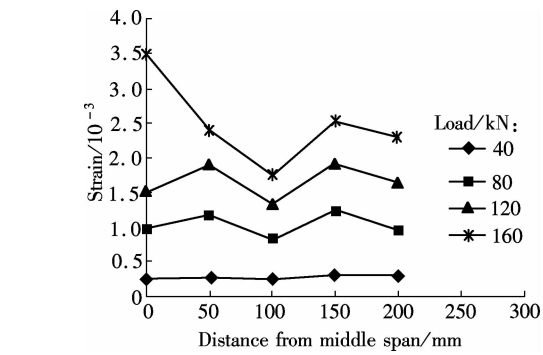

Fig. 4 Strain distributions along tensile reinforcement in pure bending region. (a) RC beam; (b) R/ECC beam

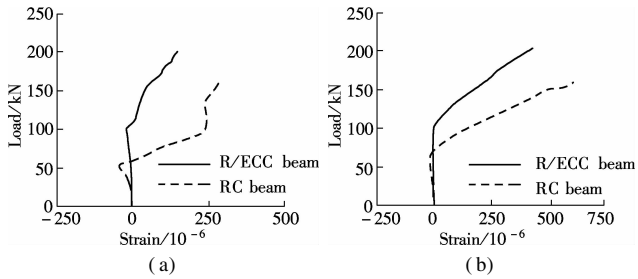

Fig. 5 Strain variations in stirrups for beam specimens. (a) Top gauge; (b) Middle gauge

3 Finite Element Simulation and Discussions

3.1 Stress-strain relationships

The finite element software ATENA is adopted to conduct numerical simulation of the beams. For the ECC, typical stress-strain curves obtained from uniaxial tension and compression tests are shown as dotted lines in Fig. 6[12-13]. To simplify numerical modelling, the stress-stain relationships of ECC, steel bars and concrete are described in Figs. 6, 7 and 8, respectively.

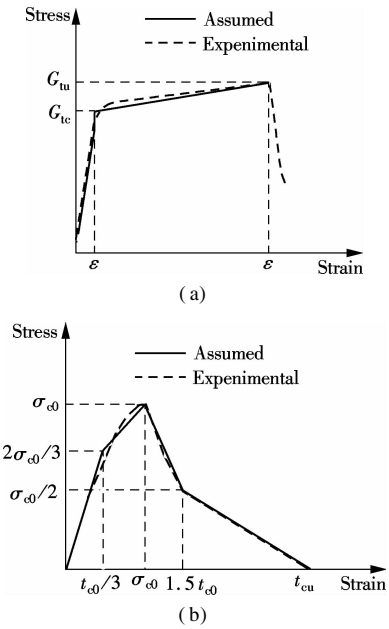

Fig. 6 Stress-strain relationship of ECC. (a) Under uniaxial tension; (b) Under uniaxial compression

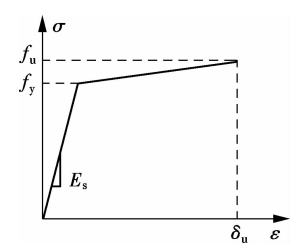

Fig. 7 Stress-strain relationship of steel bars

3.2 Finite element model

According to the symmetry of the beam about its vertical axis, half of the beam model is set up for numerical

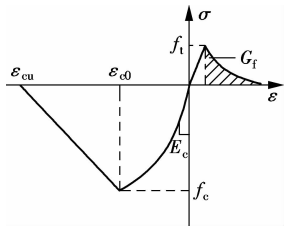

Fig. 8 Stress-strain relationship of concrete

analysis. The mid-span section is fixed at the longitudinal direction. The longitudinal reinforcement is modelled with truss elements. In this analysis, the beams were loaded by displacement control during the loading process. The Newton-Raphson iterative procedure is selected as the solution method. Both displacement and residual convergence criteria are adopted in the computation and the error tolerance is set to be 0.01. Tab. 3 and Tab. 4 show the material parameters of concrete and ECC, which are obtained from the uniaxial test results.

Tab. 3 Material properties of concrete

Compressive strength/MPa	Compressive strain at peak stress	Crushing strain	Elastic modulus/GPa	Tensile strength/MPa	Fracture energy/(N · m^{-1})
46.2	0.002	0.003 8	32.95	3.26	81.43

Tab. 4 Material properties of ECC

First cracking strength/MPa	First cracking strain/10^{-3}	Ultimate tensile strength/MPa	Ultimate tensile strain	Compressive strength/MPa	Compressive strain at peak stress	Ultimate compressive strain
3	0.21	4.5	0.03	38.3	0.004	0.12

3.3 Simulation results and discussion

The comparison of load-deflection curves between the experimental and simulation results are shown in Fig. 9. For the RC beam, the predicted curve can be divided into two stages. The predicted load first increases linearly with the corresponding deflection before the yield strength reaches 168.6 kN. After that, the curve suddenly changes and keeps almost horizontal until the ultimate moment is reached. The maximum deflection of 65.9 mm is reached with the crushing of concrete in the compression zone. For the ECC beam, the applied load drops abruptly after the maximum load carrying capacity is obtained. According to the simulation results, this softening stage corresponds to the compressive softening period of the ECC after the peak stress is reached. After that, a large deflection occurs with the load increasing slightly. In general, the predicted results show reasonable agreement with the measured results.

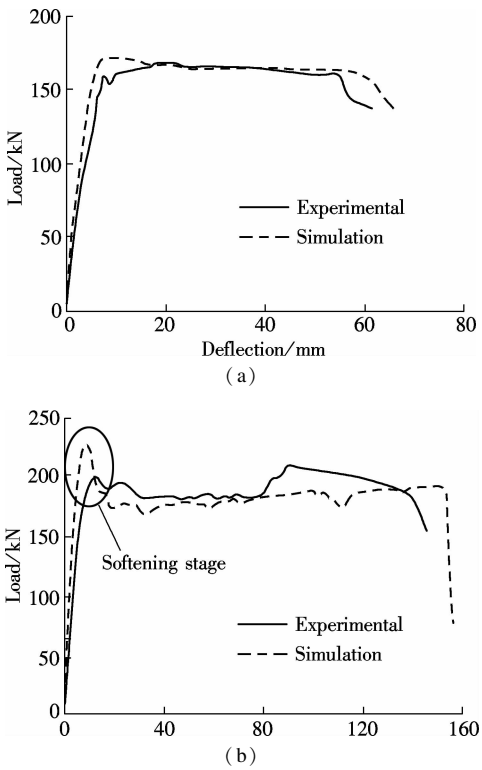

Fig. 9 Comparisons of load-deflection curves between simulation and test results. (a) RC beam; (b) R/ECC beam

Fig. 10 shows the maximum crack width vs. mid-span deflection curves of specimens at the first 15 load steps. For the RC beam, the crack width increases almost linearly with deflection. For the R/ECC beam, the increase of crack width slows down with the increasing deflection of the beam, and finally the maximum crack width keeps constant of about 0.4 mm. The significant difference in crack width development is derived from the different cracking processes of concrete and the ECC. For conventional concrete, tension-softening process occurs once its tensile strength is obtained. However, for ECC materials, after the first cracking, tensile load continues to increase with strain hardening behaviour accompanied by multiple cracks. For each individual crack, the crack

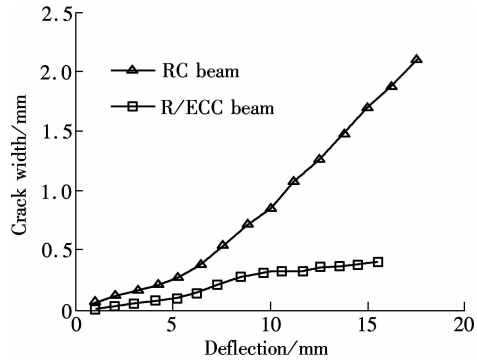

Fig. 10 Maximum crack width vs. deflection curves at the first 15 load steps (1 mm/step)

tends to open steadily up to a certain crack width, and the increasing deformation will result in a formation of an additional crack. With the same cracking mechanism, cracking of the ECC member can reach a saturated state with small crack spacing until the localization of a random single crack occurs.

Fig. 11 shows the strain distributions along the tensile steel bars at different stages. Both the beams are at the elastic stage with the deflection of 1 mm, and the strain distributions of the two beams distribute uniformly along the longitudinal bar. Cracks occur in the pure moment region with the deflection of 5.3 mm, and the stresses carried by the concrete transfer to the reinforcing bars, resulting in a sudden increase in the strains of steel reinforcement at the cracked sections. However, for the ECC beam, the stresses can be undertaken by the ECC due to the fiber bridging effect after cracking, and multiple tiny cracking of the ECC has little effect on its tensile strength. Hence, the strains along the longitudinal reinforcement distribute uniformly on the R/ECC beam. Large cracks occur in the RC beam with the deflection of 7.5 mm, and the maximum strain of the steel reinforcement is 5.838×10^{-3}, which is about 0.57 times larger than those of the R/ECC beam (3.720×10^{-3}).

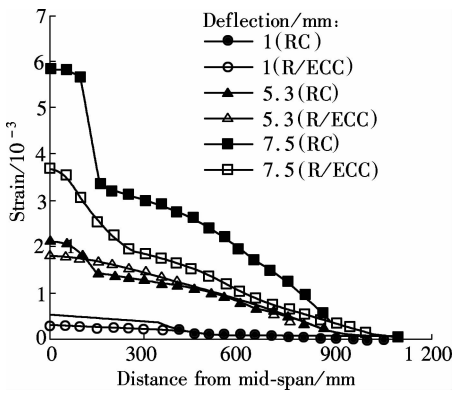

Fig. 11 Strain distributions along the tensile steel bars at different stages

4 Conclusion

In this paper, a pair of steel reinforced beams with different matrix types are tested in flexure. The flexural strength and ductility of the R/ECC beam are 24.8% and 187.67% times greater than those of the RC beam. According to the strain analysis, it can be concluded that the strains of the R/ECC beam are distributed more uniformly along the longitudinal reinforcement than those of the RC beam, and the average stirrup strain for the R/ECC beam is much smaller than that of the RC beam at the same load value.

A simplified constitutive model of ECC material is applied to simulate the flexural behaviours of beams by the finite element method. The simulation results show a good agreement with the test results. Based on the simulation results, the strains along the longitudinal reinforcement distribute smoothly for the R/ECC beam due to the compatible deformation between steel reinforcement and the ECC. The cracking patterns of the two beams are also clearly different. Instead of a few large opening cracks observed on the RC beam, numerous small cracks are observed on the R/ECC beam. The crack width of the R/ECC beam is limited to 0.4 mm under service load conditions. In summary, for flexural members, the substitution of concrete with ECC can significantly increase the flexural performance in terms of flexural strength, deformation capacity and ductility.

References

[1] Li Z J. *Advanced concrete technology* [M]. Jersey, USA: John Wiley & Sons Inc., 2011.

[2] Li V C. On engineering cementitious composites (ECC) [J]. *Journal of Advanced Concrete Technology*, 2003, **1**(3): 215 - 229.

[3] Kim Y Y, Fischer G, Li V C. Performance of bridge deck link slabs designed with ductile ECC [J]. *ACI Structural Journal*, 2004, **101**(6): 792 - 801.

[4] Lepech M D, Li V C. Application of ECC for bridge deck link slabs [J]. *Materials and Structures*, 2009, **42**(9): 1185 - 1195.

[5] Yang E H, Li V C. Tailoring engineered cementitious composites for impact resistance [J]. *Cement and Concrete Research*, 2012, **42**(8): 1066 - 1071.

[6] Canbolat B A, Parra-montesinos G J, Wight J K. Experimental study on the seismic behavior of high-performance fiber reinforced cement composite coupling beams [J]. *ACI Structural Journal*, 2005, **102**(1): 159 - 166.

[7] Fischer G, Li V C. Effect of matrix ductility on deformation behavior of steel reinforced ECC flexural members under reversed cyclic loading condition [J]. *ACI Structural Journal*, 2002, **99**(6): 781 - 790.

[8] Parra-montesinos G J, Wight J K. Seismic response of exterior RC column-to-steel beam connections [J]. *Journal of Structural Engineering*, 2000, **126**(10): 1113 - 1121.

[9] Kesner K E, Billington S L. Investigation of infill panels made from engineered cementitious composites for seismic strengthening and retrofit [J]. *Journal of Structural Engineering*, 2005, **131**(11): 1712 - 1720.

[10] Fisher G, Li V C. Intrinsic response control of moment-resisting frames utilizing advanced composite materials and structural elements [J]. *ACI Structural Journal*, 2003, **100**(2): 166 - 176.

[11] Billington S L, Yoon J K. Cyclic response of unbonded posttensioned precast columns with ductile fiber-reinforced concrete [J]. *Journal of Bridge Engineering*, 2004, **9**(4): 353 - 363.

[12] Leung C K Y, Cao Q. Development of pseudo-ductile permanent formwork for durable concrete structures [J]. *Materials and Structures*, 2010, **43**(7): 993 - 1007.

[13] Cai X R, Xu S L. Uniaxial compressive properties of ultra high toughness cementitious composite [J]. *Journal of Wuhan University of Technology: Material Science*, 2011, **26**(4): 1 - 11.

钢筋增强 ECC 梁受弯性能的试验及数值研究

蔡景明　潘金龙　袁　方

（东南大学混凝土及预应力混凝土教育部重点实验室，南京 210096）

摘要：为了研究钢筋增强 ECC 梁受弯性能，进行了钢筋增强 ECC 梁和普通钢筋混凝土梁受弯的对比研究. 结果表明，相比普通钢筋混凝土梁，钢筋增强 ECC 梁的受弯承载力和延性分别提高了 24.8% 和 187.76%，并且在梁中用 ECC 代替混凝土可有效延缓裂缝的发展. 此外，采用简化的 ECC 本构模型对钢筋增强 ECC 及混凝土梁的受弯性能进行了非线性有限元分析，模拟结果与试验结果吻合较好，在服役期间钢筋增强 ECC 梁的裂缝可以控制在 0.4 mm 以下. ECC 材料的使用可明显提高梁的抗弯承载力、变形能力、延性等受弯性能.

关键词：高延性纤维增强水泥基复合材料；延性；受弯性能；有限元

中图分类号：TU375